Hindawi
Advances in Astronomy
Volume 2024, Article ID 5786292, 13 pages
https://doi.org/10.1155/2024/5786292

Research Article

Tracking and Disturbance Suppression of the Radio Telescope Servo System Based on the Equivalent-Input-Disturbance Approach

Lei Yang[1,2], **Na Wang**[1,3], **Zhiyong Liu**[1,3] **and Ning Li**[1,3]

[1]*Xinjiang Astronomical Observatory, Chinese Academy of Sciences, Urumqi 830011, China*
[2]*University of Chinese Academy of Sciences, Beijing 100049, China*
[3]*Key Laboratory of Radio Astronomy, Chinese Academy of Sciences, Nanjing 210008, China*

Correspondence should be addressed to Na Wang; na.wang@xao.ac.cn

Received 4 October 2023; Revised 8 February 2024; Accepted 29 February 2024; Published 8 March 2024

Academic Editor: J. R. K. Kumar Dabbakuti

This paper presents a composite control algorithm for the radio telescope servo control system to address the target tracking and matched/mismatched disturbance suppression problems. The algorithm consists of the equivalent-input-disturbance (EID) approach and the optimal control method. An EID estimator is developed using the difference between the estimated output of the state observer and the measurement output and then the estimate of the EID is fed forward into the control input to reject the disturbance. A cost function with clear physical meaning is selected and the weighting parameters are adjusted for the optimal controller to improve tracking performance. Considering the nonminimum phase characteristics of the radio telescope system, the state observer gain is computed using the linear matrix inequality (LMI) method. The system stability is analyzed using the small gain theorem, and the linear quadratic regulator (LQR) control method is utilized to determine the state feedback gain. Finally, the composite controller is designed for an identified telescope model. Simulation results show that for the tracking performance, the settling time of proposed method is 1.13 s and reduces by about 0.32 s and 0.87 s than that of the ADRC controller and PI controller, respectively. For the antidisturbance performance, the RMS value and the maximum error of the proposed method are 0.0039 and 0.0128, which are 42.86% and 40.38% of the ADRC controller and 30.71% and 27.77% of the PI controller, respectively, which indicates that the proposed method has better control performance. In addition, the proposed controller has certain robustness to systematic parameter perturbations.

1. Introduction

Radio telescopes play a crucial role in collecting radio waves emitted by celestial objects [1]. Sensitivity and spatial angular resolution are important indicators for measuring the performance of a radio telescope. Increasing the aperture of the reflecting surface is the main way to improve those indicators of the telescope [2], such as the 110 m Qitai radio telescope (QTT) aims to allow high-sensitivity observations from 150 MHz up to 115 GHz [3]. However, this leads to a decrease in the mechanical resonant frequency of the antenna [4]. In addition, the transfer function from the motor's output torque to the displacement at the end of the flexible structure always displays the characteristics of the nonminimum phase [5], which makes the design of the antenna's servo controllers challenging.

The primary function of the antenna is to locate and continuously track targets accurately. As a result, the servo system of the antenna should possess high tracking accuracy, excellent transient performance, and strong resistance to disturbances. However, radio telescopes are typically located in outdoors and are susceptible to external disturbances such as wind gusts and temperature fluctuations [6]. These factors can increase the difficulty of designing antenna servo system controllers.

Currently, the main control algorithm used in the antenna servo control system is the proportional-integral-derivative (PID) controller. While the PID controller is easy

to adjust and has a simple structure, it is insufficient for meeting the high-frequency observation requirements of large aperture telescopes. With the development of the control theory, linear quadratic Gaussian (LQG) control [7, 8] and H_∞ control [9] have been successfully applied to improve the tracking and antidisturbance performance of the antenna. However, LQG control requires an accurate mathematical model and lacks robustness [10], while H_∞ control sacrifices control performance for increased robustness [11]. In addition, these control algorithms are single degree of freedom and there is a tradeoff between tracking performance and disturbance suppression [12].

The active disturbance compensation method has two degrees of freedom, one degree is used to estimate and compensate for the disturbances and the other is designed to achieve the expected control performance. The sliding mode controller and its improvements, combined with some observers, have been applied to flexible joint robots to improve their tracking performance and antidisturbance performance [13–16]. However, the design of the controllers is very complex. Active disturbance rejection control (ADRC) has been successfully applied to improve the control performance of the telescope servo system [17, 18]. However, standard ADRC is limited to integral chain systems [19], and the extended state observer (ESO) can only tackle slowly varying disturbances [20]. A disturbance observer-based composite position controller (DOB-CPC) is designed to enhance antidisturbance capability of Leighton Chajnantor telescope [21]. A cascade acceleration feedback control (AFC) enhanced by disturbance observation and compensation is proposed to improve the tracking precision of telescope systems [22]. However, the DOB mainly estimates input disturbances and requires the inverse model of the system, which may destroy the system's stability when the plant is a nonminimum phase system [23].

Another active disturbance rejection method is the equivalent input disturbance (EID) approach [24]. The fundamental concept is to define an EID in the control input channel which has the same impact on the system output as external disturbances, estimate the EID using an EID estimator, and then introduce the estimated EID into the input channel to compensate for the external disturbance. The EID approach does not require the inverse model of the system and can compensate for many kinds of unmeasurable disturbances, no matter if it is matched or mismatched. It has been successfully applied to time-delay systems [25], nonlinear systems [26], and linear uncertain systems [27]. What is more, some improved methods were developed to enhance the antidisturbance performance of the EID approach. For example, dynamic compensator and high-order low-pass filter were introduced to improve the disturbance rejection performance [28, 29]. Unlike the disturbance observer and the feedback controller are designed simultaneously to guarantee the closed system robust stability [30, 31], the EID-based control method has an important feature; the state-feedback control law can be designed independently of the observer gain and the disturbance estimator when stability is the only concern [24]. Also, the EID approach can compensate for the uncertainties and disturbances, so the designed controller has certain robustness [32].

Applying the EID method to the antenna servo control system can improve the antenna's antidisturbance ability under unknown disturbances. However, the antenna servo system is a nonminimum phase system, and the perfect regulation method used in [28, 29] cannot be applied to obtain the observer gain. In addition, the method presented in [33] is too complex and needs solving three inequalities.

Based on these considerations, this paper proposes a new parameter design method for the antenna servo controller based on the EID approach. To resolve the nonminimum phase characteristic of the antenna system model, the LMI method based on the bounded real lemma is proposed to obtain the state observer gain. To simplify the problem of difficulty in selecting weight parameters in optimal control, the weighting parameters of a cost function with clear physical meaning are adjusted to get an optimal controller using the LQR control method. The EID estimator is also designed for disturbance rejection, and the system's stability is analyzed using the small gain theorem.

The primary contributions of this paper are as follows:

(1) Utilizing a composite control algorithm with the EID approach and the optimal control method can enhance the tracking performance, suppressing matched and mismatched disturbances of the antenna servo system.

(2) Unlike the methods used in [25, 28, 29], this paper proposes a cost function with clear physical meanings and achieves satisfactory tracking performance using the LQR control method by adjusting the weighting parameters.

(3) The proposed method of using the LMI technique to get observer gain is very simple and can apply to minimum-phase and nonminimum-phase systems.

The remaining sections of the paper are organized as follows. Section 2 outlines the antenna model and controller structure. In Section 3, the stability of the closed system, based on the separation theorem, is analyzed, and a method for designing the controller parameters is proposed. Section 4 presents simulation results on an antenna servo system to demonstrate the effectiveness of the proposed method. Finally, Section 5 provides conclusions.

2. Antenna Model and Controller Structure

2.1. Antenna Model Analysis. The servo control system of a radio telescope is a typical electromechanical system that consists of driving motors, a reducer, a main reflector, and a feedarm supporting subreflector. In the service mode, the reflector is driven by the azimuth axis and elevation axis motors to ensure the accuracy of pointing and tracking. Figure 1 shows the structure of a fully steerable radio telescope.

As the aperture increases, the structure of the telescope servo system becomes more flexible and complex, making it difficult to model using the traditional mechanism modeling method. We can obtain a close approximation model of the actual antenna by employing system identification methods. Since the azimuth and elevation axes of the antenna are

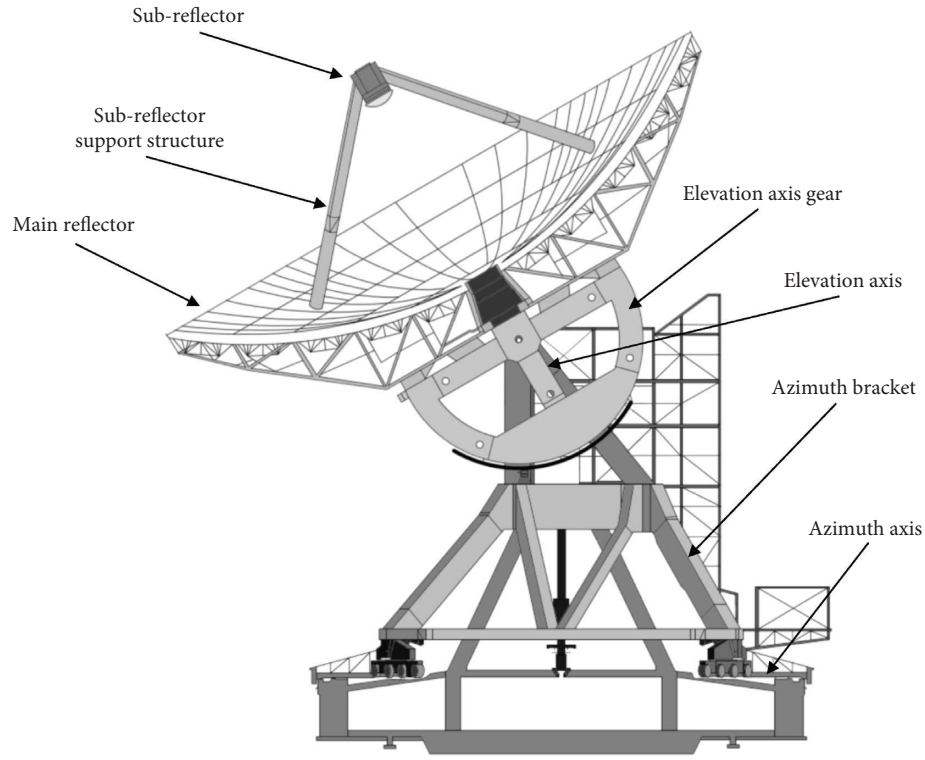

Figure 1: Diagram of the structure of a fully steerable radio telescope.

orthogonal, which results in minimal coupling between the two systems [17, 34], this allows us to treat them as independent subsystems. In the paper, we focus on identifying the azimuth axis position open-loop system and designing a position loop controller.

Figure 2 shows the structure of the azimuth axis system used for identification experiments. The antenna model includes the drive model and the antenna structure. The speed loop corrected by the speed controller has good dynamic characteristics, which can be described using a first-order transfer function, namely,

$$G_m = \frac{1}{T_m s + 1}, \tag{1}$$

where T_m is the time constant of the speed loop. The antenna structure can be described by a transfer function G_a

$$G_a = \frac{b_0 + b_1 s + b_2 s^2 + \cdots + b_m s^m}{a_0 + a_1 s + a_2 s^2 + \cdots + a_m s^m}, \tag{2}$$

where a_i and b_i, $i = 0, 1 \ldots m$, $m > 0$, are to be determined parameters. Then, the whole antenna model can be described as

$$G = \frac{1}{T_m s + 1} \frac{b_0 + b_1 s + b_2 s^2 + \cdots + b_m s^m}{a_0 + a_1 s + a_2 s^2 + \cdots + a_m s^m}. \tag{3}$$

Equation (3) can be described by $G = C(sI - A)^{-1}B$, where A, B, and C are the state matrix, input matrix, and output matrix. Through the system identification experiment, the parameters A, B, and C can be obtained. Then, we can get the following state space equation to describe the dynamic model of the radio telescope.

$$\begin{cases} \dot{x}(t) = Ax(t) + Bu(t), \\ y(t) = cx(t), \end{cases} \tag{4}$$

where $A \in \mathbb{R}^{n \times n}$, $B \in \mathbb{R}^{n \times 1}$, $C \in \mathbb{R}^{1 \times n}$, $x(t) \in \mathbb{R}^n$, $u(t) \in \mathbb{R}$, and $y(t) \in \mathbb{R}$. $x(t)$, $u(t)$, and $y(t)$ are, respectively, the state vectors, the control input, and the measurement output.

2.2. Structure of the EID-Based Controller. Since the antenna system is affected by different types of disturbances and most of the disturbances do not enter the system through the input channel, the system model and the disturbances can be described by`

$$\begin{cases} \dot{x}(t) = Ax(t) + Bu(t) + B_d d(t), \\ y(t) = cx(t), \end{cases} \tag{5}$$

where $B_d \in \mathbb{R}^{n \times 1}$, $d(t) \in \mathbb{R}$. If $B = \lambda B_d, \lambda \in \mathbb{R}$, the disturbance is a matched one; otherwise, it is mismatched.

Assumption 1. The state of system (5) is fully controllable and observable, and the controlled object has no zeros at the origin.

Remark 2. The controllability ensures that the designed system is stable, observability is necessary for designing the system state observer, and having no zeros at the origin ensures that the system can accurately track a step signal without any steady-state error.

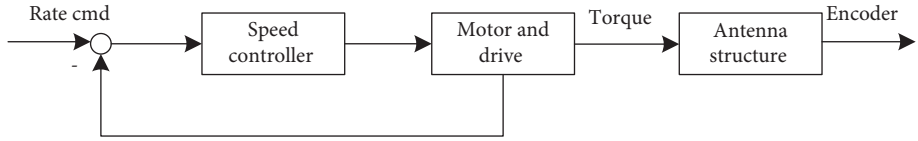

Figure 2: The configuration of the antenna for the identification experiment.

The system block diagram of the radio telescope servo system, based on the EID approach, is presented in Figure 3. The designed controller consists of internal model control, state feedback gain, Luenberger state observer, and an EID estimator.

As seen in the literature [24], there is an EID, $d_e(t)$, in the input channel which generates the same output as the unknown mismatched disturbance for the system. Consequently, system (5) can be converted into

$$\begin{cases} \dot{x}(t) = Ax(t) + B[u(t) + d_e(t)], \\ y(t) = Cx(t). \end{cases} \tag{6}$$

A Luenberger state observer is constructed to estimate the $d_e(t)$,

$$\begin{cases} \dot{\hat{x}}(t) = A\hat{x}(t) + Bu_f(t) + L(y(t) - \hat{y}(t)), \\ \hat{y}(t) = C\hat{x}(t), \end{cases} \tag{7}$$

where $\hat{x}(t)$ is the estimate of the system state, $\hat{y}(t)$ is the estimated output, and L is the state observer gain. Defining the state observation error as

$$\Delta x(t) = x(t) - \hat{x}(t), \tag{8}$$

and incorporating it in (5) yields

$$\dot{\hat{x}}(t) = A\hat{x}(t) + Bu(t) + Bd_e(t) + A\Delta x(t) - \Delta\dot{x}(t). \tag{9}$$

Assuming there exists $B\Delta d(t) = A\Delta x(t) - \Delta\dot{x}(t)$, let

$$\hat{d}(t) = d_e(t) + \Delta d(t), \tag{10}$$

and by combining equations (7)–(10), it can be concluded that

$$\hat{d}(t) = B^{+}LC\Delta x(t) + u_f(t) - u(t), \tag{11}$$

where B^{+} is the Moore–Penrose generalized inverse of B, namely, $B^{+} = (B^{T}B)^{-1}B^{T}$.

Since the EID estimate $\hat{d}(t)$ may be influenced by measured noise and there is a causal relationship between $\hat{d}(t)$ and the control input $u(t)$, a first-order low-pass filter,

$$F(s) = \frac{1}{Ts + 1}, \tag{12}$$

is designed to solve these problems. And, $F(s)$ should satisfy

$$F(j\omega) \approx 1, \quad \forall\omega \in [0, \omega_d], \tag{13}$$

where ω_d is the maximum angular frequency of the external disturbance. The cutoff frequency of the low-pass filter is generally chosen as $1/T \geq 5\omega_d$. And then,

$$\tilde{D}(s) = F(s) * \hat{D}(s), \tag{14}$$

where $\hat{D}(s), \tilde{D}(s)$ are the Laplace transforms of $\hat{d}(t), \tilde{d}(t)$.

For the tracking performance of the radio telescope, based on the reference signal of the system, the internal model is obtained as

$$\dot{x}_i(t) = A_i x_i(t) + B_i(r(t) - y(t)), \tag{15}$$

where $r(t)$ and $y(t)$ are the reference input and the measurement output, A_i, B_i are the constant matrices, and x_i is the state. The internal model is used to guarantee zero-error tracking performance in the steady state.

By designing the state feedback of the system, the control law of the whole system is finally obtained as

$$u(t) = u_f(t) - \tilde{d}(t), \tag{16}$$

where

$$u_f(t) = K_i x_i(t) + K_p\hat{x}(t), \tag{17}$$

where K_p, K_i is the state feedback gain of the system.

3. Stability Analysis and Controller Parameters Design

3.1. Stability Analysis of Closed-Loop System. Stability is the inherent property of linear systems and is independent of external signals. Therefore, let $r(t) = 0$ and $d(t) = 0$, then the system (5) is transformed to (4). Based on the above equation and equations (7), (8), (11), and (16), we get

$$\begin{cases} \Delta\dot{x}(t) = (A - LC)\Delta x(t) - B\tilde{d}(t), \\ \tilde{d}(t) = B^{+}LC\Delta x(t) + \tilde{d}(t). \end{cases} \tag{18}$$

Then, the transfer function from $\tilde{d}(t)$ to $\hat{d}(t)$ is

$$\begin{aligned} G(s) &= 1 - B^{+}LC(sI - (A - LC))^{-1}B \\ &= B^{+}(sI - A)(sI - (A - LC))^{-1}B. \end{aligned} \tag{19}$$

The above equation suggests that the state feedback gain is independent of the observer gain. According to the separation theorem, the state feedback gain and the observer gain can be independently designed. As shown in Figure 4 which is equivalently converted from Figure 3, the control system is divided into two subsystems; one with the state feedback gain and internal model and the other with an EID estimator and the $G(s)$.

For subsystem 1, according to the small gain theorem, if the system is stable, it should satisfy

$$\|F(s)G(s)\|_{\infty} < 1. \tag{20}$$

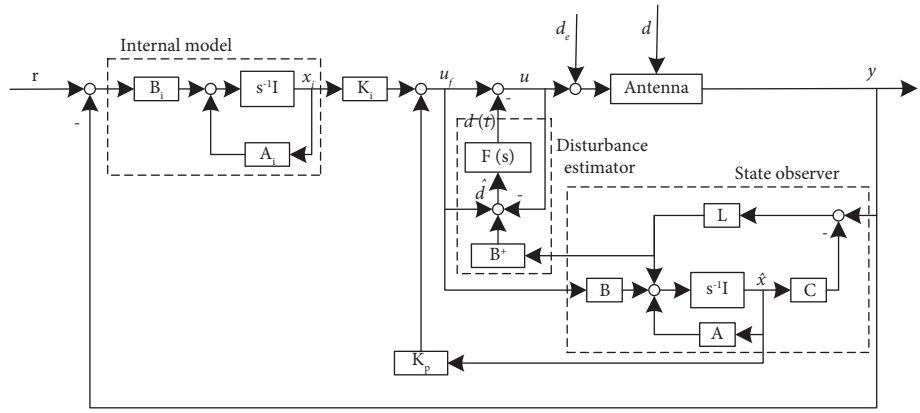

Figure 3: Configuration of the antenna control system based on the EID approach.

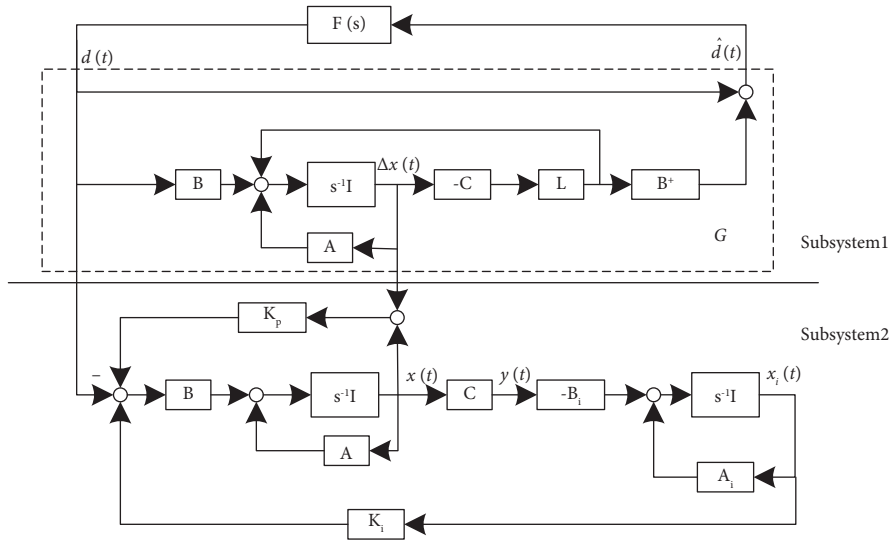

Figure 4: Equivalent diagram of the control system based on the EID approach.

Based on the above analysis, we can get the following theorem:

Theorem 3. *System (5) satisfies Assumption 1, and the designed system satisfies the following conditions [35]:*

(a) $A + BK_p$ *is a Hurwitz matrix;*

(b) $A - LC$ *is a Hurwitz matrix;*

(c) $\|F(s)G(s)\|_\infty < 1$;

then, the whole control system designed by the EID approach and the optimal control method is asymptotically stable.

Proof. Since the EID-based system can be decomposed into two subsystems (subsystem 1 and subsystem 2), the stability of the whole system is equivalent to that of these two subsystems. For the subsystem 1, it is composed of $G(s)$ and $F(s)$. First, $G(s)$ and $F(s)$ should be stable, and the condition (2) must be held. According to the small gain theorem, the subsystem 1 is stable if condition (3) holds. For the subsystem 2, it is a state feedback control system, when the state feedback gain $[K_p\ K_i]$ has been designed, and the subsystem 2 is stable if condition (1) holds. □

3.2. Controller Parameters Design. The out-loop controller of the system is composed of the internal model and optimal state feedback, which is designed through the LQR control method. The generalized controlled plant is described as

$$\begin{cases} \dot{\bar{x}}(t) = \overline{A}\bar{x}(t) + \bar{B}u(t), \\ y(t) = \bar{C}\bar{x}(t), \end{cases} \tag{21}$$

where

$$\overline{x}(t) = \begin{bmatrix} x(t), \\ x_i(t). \end{bmatrix}, \overline{A} = \begin{bmatrix} A & 0 \\ -B_iC & A_i \end{bmatrix}, \overline{B} = \begin{bmatrix} B \\ 0 \end{bmatrix}, \overline{C} = [C \quad 0]. \tag{22}$$

Design the control law, $u(t) = \begin{bmatrix} K_p & K_i \end{bmatrix} \begin{bmatrix} x(t) \\ x_i(t) \end{bmatrix}$, to find the control input that minimizes a cost function. Select a target output as

$$z = \left[\, y \;\; r_0 \dot{y} \;\; r_1 x_i \,\right]^T, \tag{23}$$

where y is the position output of the system; $\dot{y}$ is the speed of the output that means how fast the system can reach the inference input; x_i is the integration of the residual between the reference input signal and the output signal, which reflects the tracking performance of the system; and r_0 and r_1 are the weight coefficient. The cost function of the system is designed as

$$J = \int_0^\infty \left[\|z(t)\|^2 + \rho\|u(t)\|^2\right] \mathrm{d}t. \tag{24}$$

Adjust r_0, r_1, and ρ, and use the LQR control method to obtain state feedback gains K_p, K_i to meet the tracking performance.

The servo control system of the radio telescope has nonminimum phase characteristics. However, the perfect regulation method [36] is only applicable to the minimum phase system. Therefore, in this paper, we utilize the LMI method based on the bounded real lemma to calculate the observer gain. This method is suitable for both minimum-phase and nonminimum-phase systems.

Lemma 4 (Bounded real lemma [37]). *For a continuous system, a minimum realization is*

$$\begin{cases} \dot{x}_s(t) = A_s x_s(t) + B_s u_s(t), \\ y_s = C_s x_s(t) + D_s u_s(t), \end{cases} \tag{25}$$

where $A_s \in R^{n\times n}$, $B_s \in R^{n\times m}$, $C_s \in R^{p\times n}$, and $D_s \in R^{p\times m}$ are the system matrices. If there is a positive definite symmetric matrix P that satisfies

$$\begin{bmatrix} A_s^T P + P A_s & P B_s & C_s^T \\ * & -I & D_s^T \\ * & * & -\gamma^2 I \end{bmatrix} < 0, \tag{26}$$

then the system G_s is stable and $\|G_s\|_\infty < \gamma$. Note: $\begin{bmatrix} A_1 & A_2 \\ * & A_3 \end{bmatrix} = \begin{bmatrix} A_1 & A_2 \\ A_2^T & A_3 \end{bmatrix}$.

For the dual system of (5),

$$\begin{cases} \dot{x}_1(t) = A^T x_1(t) + C^T u(t) + C^T w(t), \\ y_1(t) = B^T x_1(t), \end{cases} \tag{27}$$

where $w(t)$ is a virtual external signal of the dual system. By designing a control law $u(t) = -L^T x_1(t)$ and integrating it into equation (25), the transfer function from the input $w(t)$ to the output $y_1(t)$ can be obtained as

$$G_1(s) = B^T\left(sI - \left(A^T - C^T L^T\right)\right)^{-1} C^T. \tag{28}$$

By comparing equations (19) and (28), we find that the amplitude change of $G_1(s)$ has impact on the amplitude of $G(s)$, thereby allowing us to obtain the state observer gain that satisfies the stability conditions in Theorem 3. The following theorem outlines how to derive the gain of the state observer using the bounded real lemma.

Theorem 5. *For a continuous system, the minimum realization is*

$$\begin{cases} \dot{x}_e(t) = A_e x_e(t) + B_e u(t) + B_w w(t), \\ y(t) = C_e x_e(t) + D_e u(t) + D_w w(t), \\ u(t) = K_e x_e(t), \end{cases} \tag{29}$$

where $A_e \in \mathbb{R}^{n\times n}$, $B_e \in \mathbb{R}^{n\times 1}$, $C_e \in \mathbb{R}^{1\times n}$, $D_e, B_w, D_w \in \mathbb{R}$, $x_e(t) \in \mathbb{R}^n$, and $u(t), w(t), y(t) \in \mathbb{R}$. If there exists a symmetric positive definite matrix $Q \in \mathbb{R}^{n\times n}$ and a general matrix $M \in \mathbb{R}^{1\times n}$ such that

$$\begin{bmatrix} (A_e Q + B_e M) + (A_e Q + B_e M)^T & B_w & (C_e Q + D_e M)^T \\ * & -I & D_w^T \\ * & * & -\gamma^2 I \end{bmatrix} < 0, \tag{30}$$

holds, then there exists $u(t) = K_e x_e(t)$, making that the system is stable and $\|G_e\|_\infty < \gamma$, where $K_e = MQ^{-1}$ is the state feedback gain and $G_e(s)$ is the transfer function from w to y.

Proof. Based on the bounded real lemma, there exists a symmetric positive definite matrix P such that

$$\begin{bmatrix} (A_e + B_e K_e)^T P + P(A_e + B_e K_e) & P B_w & (C_e + D_e K_e)^T \\ * & -I & D_w^T \\ * & * & -\gamma^2 I \end{bmatrix} < 0, \tag{31}$$

holds, then the system is stable and $\|G_e\|_\infty < \gamma$. According to the performance criterion for linear matrix inequalities, multiplying both sides of an inequality by a positive definite matrix does not change the negative definite of the inequality. Multiplying the inequality (31) by $\mathrm{diag}\{P^{-1} \ I \ I\}$ on the left and $\mathrm{diag}\{P^{-1} \ I \ I\}^T$ on the right, respectively, yields the equivalent matrix inequality of equation (31) as follows:

$$\begin{bmatrix} A_eP^{-1} + B_eK_eP^{-1} + \left(A_eP^{-1} + B_eK_eP^{-1}\right)^T & B_w & \left(C_eP^{-1} + D_eK_eP^{-1}\right)^T \\ * & -I & D_w^T \\ * & * & -\gamma^2 I \end{bmatrix} < 0. \tag{32}$$

Let $Q = P^{-1}$ and $M = K_eQ$, then the matrix inequality (30) is obtained. □

3.3. The Controller Design Procedure. Based on the above analysis, we can achieve the following design procedure:

(1) Select a cost function, adjust the weighting parameters ρ, r_1, r_2, and get the state feedback gain $[K_p \ K_i]$, which satisfies the stability and tracking performance;

(2) Select ω_d of the external disturbance;

(3) Choose a low-pass filter that satisfies

$$F(j\omega) \approx 1, \quad \omega \in \omega_d. \tag{33}$$

(4) Adjust γ and use the method in Theorem 5 to get a suitable L, which satisfies the stability conditions (2) and (3) in Theorem 3.

4. Simulation Analysis

The Nanshan 26 m radio telescope (NSRT) is used to validate the effectiveness of the proposed approach. First, the identification experiment is carried out to obtain the model of NSRT. Then, we apply the proposed controller to the antenna servo system and analyze the performances of tracking, disturbance rejection, and robustness.

4.1. The Model of NSRT. To acquire the dynamic model of the NSRT, we use pseudorandom binary sequence (PRBS) as the input and the position encoder signal as the output. By analyzing the input data and the differential of the output data using the correlation analysis method and the eigensystem realization algorithm [38], we obtain the system parameter model.

$$G = \frac{16.16\left(s^2 + 0.8131s + 475.5\right)\left(s^2 - 35.03s + 858.6\right)\left(s^2 + 5.742s + 1016\right)}{(s + 13.59)\left(s^2 + 2.962s + 429.7\right)\left(s^2 + 1.453s + 510.2\right)\left(s^2 + 5.915s + 2107\right)}. \tag{34}$$

The Bode diagrams of the data model and identification model are present in Figure 5. It shows that the frequency characteristics of the identified system model and the data model are consistent. The Bode plot reveals that the radio telescope demonstrates the desired rigidity characteristics at frequencies below 2 Hz. However, at frequencies above 2 Hz, the system exhibits noticeable flexibility, including resonance and antiresonance peaks. By analyzing the system model, it is discovered that the system has right half plane zeros, which further complicates the controller design. The antenna position loop model is formed by adding an integrator to the identification model (34). The state space equation of the position open-loop system is

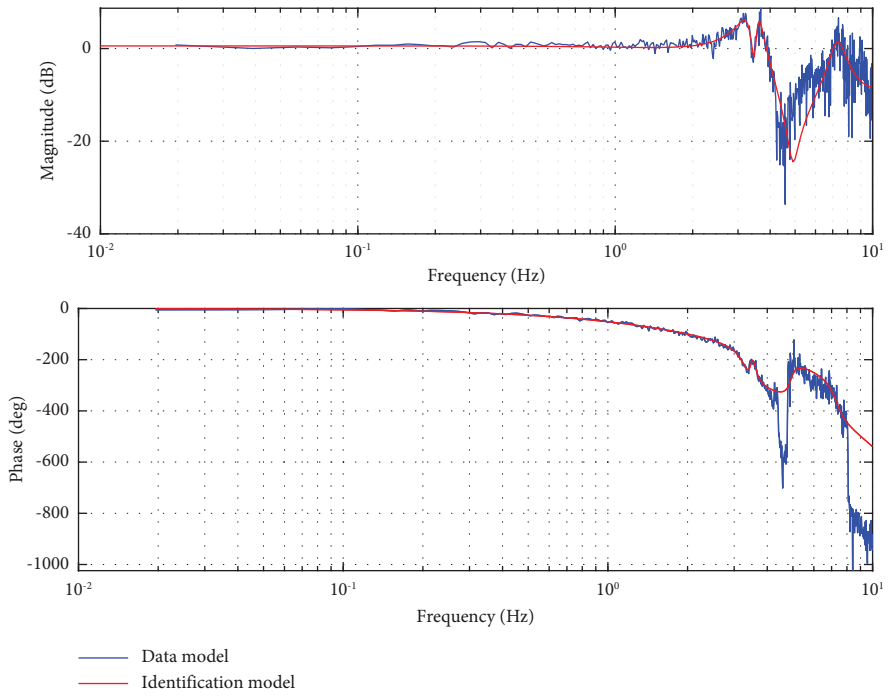

Figure 5: Bode diagrams of the plant models.

$$A = \begin{bmatrix} 0 & 0 & 0 & 0 & 0 & 0 & 0 & 0 \\ 0 & -5.73 & -15.97 & -1.78 & 0.58 & -3.67 & 3.80 & -4.88 \\ 0 & 15.97 & -3.87 & 6.01 & 0.28 & -10.64 & 2.41 & -9.13 \\ 0 & 1.78 & -6.01 & -0.76 & -21.27 & 1.60 & -5.65 & 2.39 \\ 0 & -0.58 & 0.28 & 21.27 & -0.02 & 5.76 & -0.20 & 1.40 \\ 0 & -3.67 & 10.64 & 1.60 & -5.76 & -3.40 & 16.06 & -5.14 \\ 0 & -3.80 & 2.40 & 5.65 & -0.20 & -16.06 & -1.89 & 42.41 \\ 0 & -4.88 & 9.13 & 2.39 & -1.40 & -5.14 & -42.41 & -8.25 \end{bmatrix},$$

$$B = \begin{bmatrix} 0.68 & -1.03 & 0.63 & 0.21 & -0.04 & -0.42 & -0.27 & -0.51 \end{bmatrix}^T, \quad (35)$$

$$C = \begin{bmatrix} 1.56 & 1.03 & 0.63 & -0.21 & -0.04 & 0.42 & -0.27 & 0.51 \end{bmatrix},$$

$$D = 0.$$

4.2. Controller Design and Performance Analysis. Accurate pointing is a major function of radio telescopes, and now we mainly investigate its dynamic response characteristics when tracking a step signal and the anti-disturbance performance after steady state. Based on the internal model principle, we get

$$A_i = 0, \quad B_i = 1. \quad (36)$$

To obtain the state feedback gain satisfying the tracking performance, the optimal tracking controller for the generalized controlled plant is designed by adjusting r_0, r_1, and ρ. By trial and error, we obtain

$$r_0 = 0.5, \quad r_1 = 15, \quad \rho = 1. \quad (37)$$

By using the LQR control method, the state feedback gain is obtained.

$$\begin{bmatrix} K_p & K_i \end{bmatrix} = \begin{bmatrix} 13.47 & -1.04 & 1.09 & -0.65 & 0.26 & 1.99 & -3.6 & -0.5 & -15 \end{bmatrix}. \quad (38)$$

Wind load is the main disturbance to the radio telescope. The wind spectrum exhibits significant energy values within the frequency range of 0-1 Hz. In order to assess the effectiveness of the EID estimator in mitigating disturbances, a composite disturbance consists of a step signal and various sinusoidal signals at different frequencies, as depicted in Figure 6, is introduced into the system, namely,

$$d(t) = \begin{cases} 0, & t < 5, t > 10, \\ 0.05 + 0.05(\sin(3 * t) + \sin(6 * t)) & 5 \le t \le 10. \end{cases} \tag{39}$$

The maximum angular frequency of the disturbance is ω_d = 6rad/s, then the first-order low-pass filter is selected as

$$F(s) = \frac{1}{0.032s + 1}. \tag{40}$$

The state observer gain is designed based on the dual system of (4). We adjust the parameter γ to achieve a state observer gain that satisfies the stability requirements using the method described in Theorem 5. The stability is test by examining the bode plots of $F(s)$ and $G(s)$. Figure 7 displays

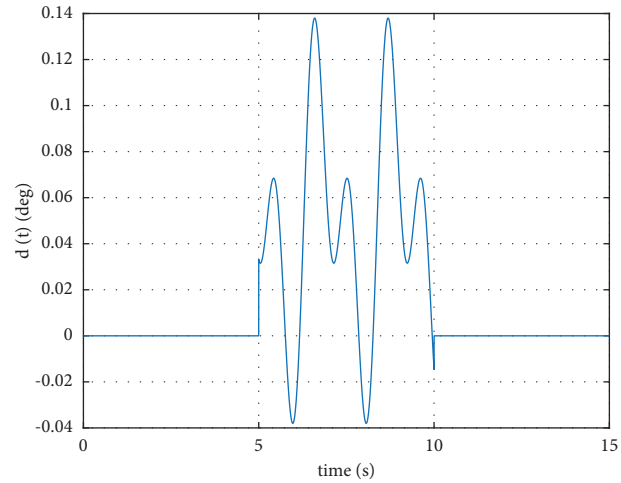

Figure 6: The external disturbance.

the Bode plots of $F(j\omega)$ and $G(j\omega)$ obtained using different values of the parameter γ. When γ = 0.15, we get

$$L = \begin{bmatrix} 1849.6 & -1335 & -1368 & -71.16 & 23.96 & -30.96 & 409.97 & -899.19 \end{bmatrix}^T, \tag{41}$$

and $\|F(s)G(s)\|_\infty = 0.9737 < 1$, which meets the stability condition in Theorem 3.

4.3. Performance Analysis. Assuming that the NSRT servo system is affected by matched and unmatched disturbances, the results of the simulation are shown in Figures 8 and 9, respectively.

At time t = 0 s, a step signal is applied to the system. Figures 8 and 9 show that regardless of whether the system includes the EID estimator, the tracking performance is the same, the system can track the reference input with almost no overshoot, and the settling time is 1.13 s. This indicates that the designed system has high tracking accuracy and excellent transient performance. After the system reaches a steady state, the disturbance is introduced to the system during t = 5–10 s. Since there is no model of the disturbance in the controller, the disturbance cannot be rejected to zero. For the matched disturbance, the maximum errors of the output caused by the disturbances are 0.0075 with the EID estimator and 0.0228 without the EID estimator. For the mismatched disturbance, they are 0.0113 and 0.0341, respectively. The system with the EID estimator exhibits better performance in rejecting disturbances compared to the system without the EID estimator.

Figure 10 shows the estimated disturbances $\widehat{d}(t)$ of matched and unmatched disturbances as well as the actual disturbance. For the estimated disturbances $\widehat{d}(t)$ of matched disturbance, there is a slight difference between them since there is $\Delta d(t)$ in equation (10). For the estimated disturbances $\widehat{d}(t)$ of mismatched disturbance, there is a large difference between them since the estimated disturbance is the estimation of the EID of mismatched disturbance.

To simplify the analysis, we focus on the worst-case scenario, in which the system is affected by a mismatched disturbance.

In order to demonstrate the advantage of the proposed method, the traditional PI controller and the ADRC controller are designed for the system. The method described in [4] is used to obtain the PI gains.

$$\begin{aligned} k_p &= 3.7, \\ k_i &= 3. \end{aligned} \tag{42}$$

Since the relative order of the antenna system is two, the ADRC consists of a three-order LESO and a PD feedback control law. Based on the method in [], the parameters are b_0 = 12, K_p = 17.25, and K_d = 11.7, and all poles of the LESO are chosen to be 24, which yielded the observer gain as follows:

$$L = \begin{bmatrix} 72 & 1728 & 13824 \end{bmatrix}, \tag{43}$$

Also, a low-pass filter is added to the control input to guarantee the control performance, which is designed as

$$F_1(s) = \frac{1}{0.125s + 1}. \tag{44}$$

The results in Figure 11 demonstrate the system performance with three different control methods. Also, the tracking performance indices are presented in Table 1. Figure 11 and Table 1 show that when the system is controlled by the PI controller, the overshoot is about 23% and the settling time is about 2 s. And, for the ADRC controller, the overshoot is about 1% and the settling time is about 1.45 s. The above analysis indicates the proposed method has better tracking performance compared to the ADRC controller and the PI controller.

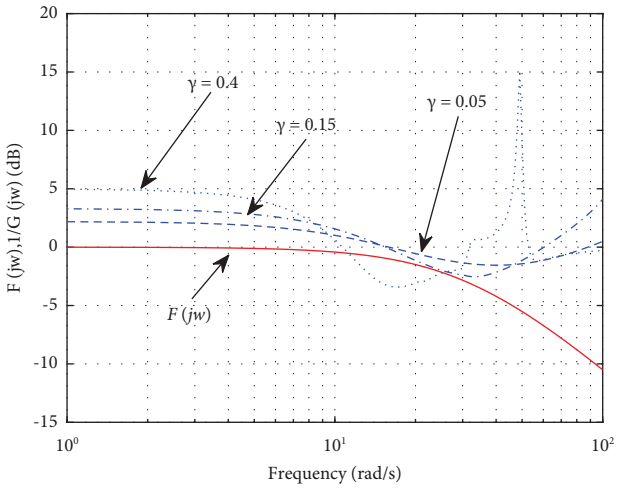

Figure 7: Bode diagrams of $F(j\omega)$ and different $G(j\omega)$.

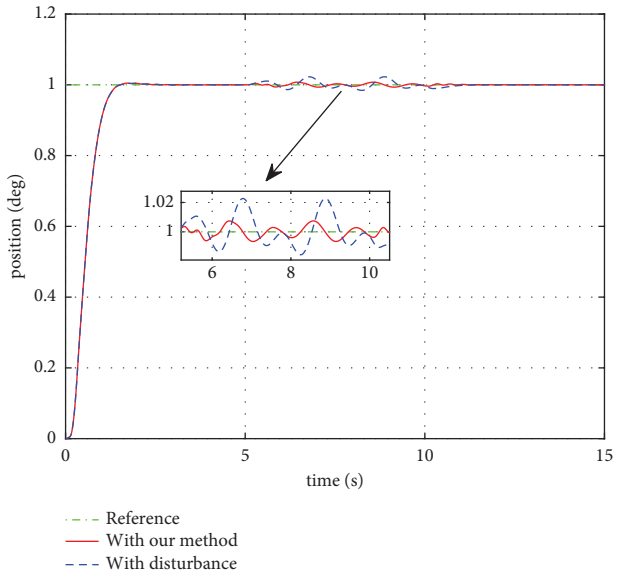

Figure 8: Output responses of the NSRT servo system with matched disturbance.

To evaluate the antidisturbance performance of the three methods, two performance indices are used, namely, the root mean square criterion (RMS) and the maximum error. The two indices are also presented in Table 1. We can get that the RMS values for the three methods are 0.0039, 0.0091, and 0.0127, while the maximum errors are 0.0128, 0.0317, and 0.0461, respectively. The RMS and maximum error value of the proposed method are 42.86% and 40.38% of the ADRC controller and 30.71% and 27.77% of the PI controller, respectively. This indicates when the EID-based controller applied to the NSRT servo system, there is a significant improvement in antidisturbance capability.

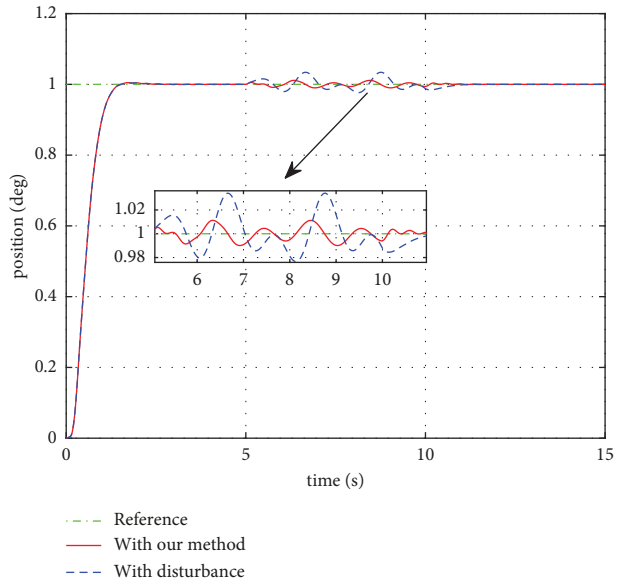

Figure 9: Output responses of the NSRT servo system with mismatched disturbance.

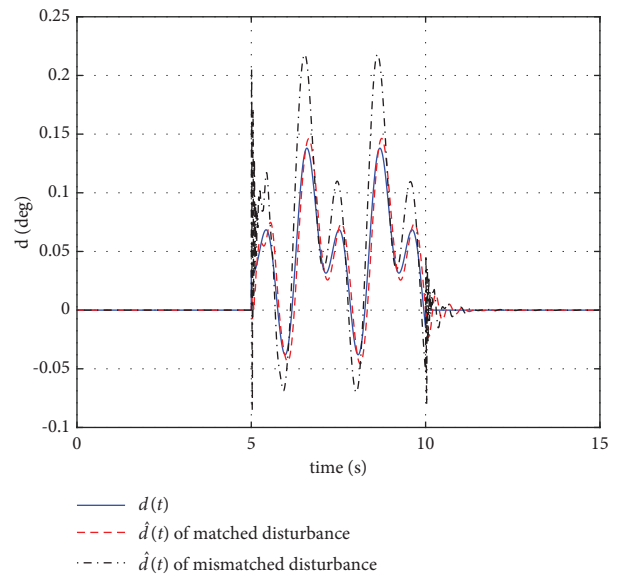

Figure 10: The actual disturbance $d(t)$ and the estimated disturbances $\hat{d}(t)$ of matched and unmatched disturbances.

The antenna servo system is always subjected to parameter uncertainty. To verify the robustness of the proposed method, it is assumed that there are parameter uncertainties in the matrices $A, B,$ and C, and the maximum perturbation is $\pm 5\%$. By randomly selecting 5 uncertainties to verify the robustness, Figure 12 shows that the tracking and disturbance rejection performance of the NSRT servo

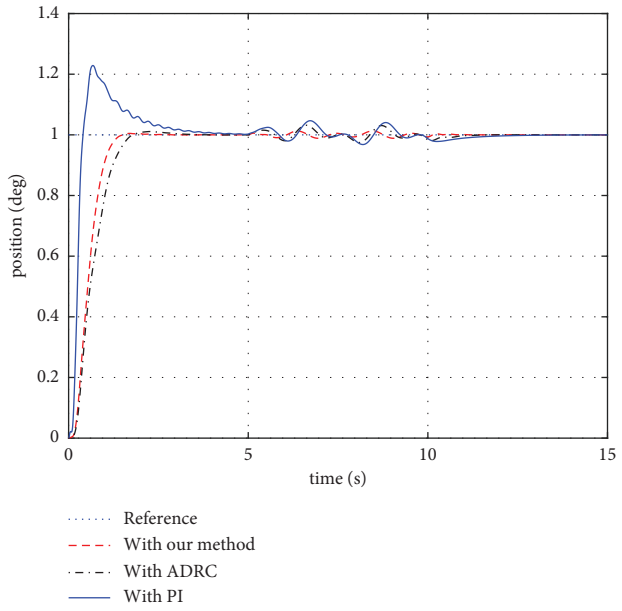

Figure 11: Comparison between the EID, ADRC, and PI.

Table 1: Tracking and antidisturbance performance of the three methods.

Methods	Overshoot	Settling time	RMS	Maximum error
Our method	0	1.13	0.0039	0.0128
ADRC	1%	1.45	0.0091	0.0317
PI	23%	2	0.0127	0.0461

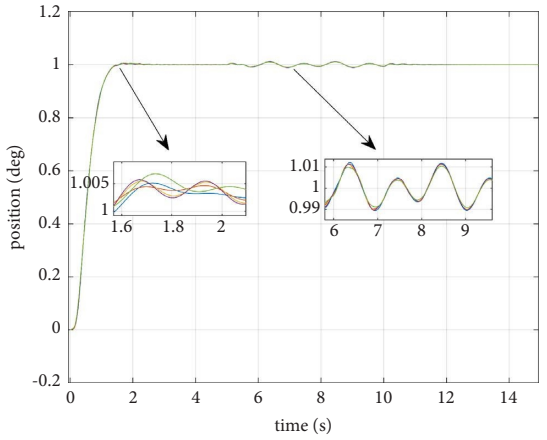

Figure 12: Responses of the NSRT servo system with parameter uncertainties.

system is not affected by the parameter perturbation, which indicates that the EID-based controller has certain robustness.

5. Conclusion

This paper introduces a composite control method to improve the tracking and disturbance suppression performance of the NSRT servo control system. The weighting parameters of the cost function with physical significance are investigated and the state feedback gain of the servo system is constructed using the LQR control method. For the nonminimum phase characteristics of the radio telescope system, the observer gain is obtained by using the LMI method, and the EID estimator is incorporated into the state feedback system to estimate and compensate for the disturbance. The simulation results show that the tracking performance of the proposed method is better than the ADRC controller and the traditional PI controller. Compared with the ADRC controller and the traditional PI controller, the RMS and the maximum disturbance-induced error in the output of the composite control method are smallest. These results indicate that the EID-based optimal control offers superior control performance.

Plans for future research are mainly in the following areas:

(1) Study the uncertainty range of the antenna servo system and apply it to the design process of the controller to further improve the robustness of the whole system.

(2) Combine the EID approach and other advanced control methods, such as MPC and SMC, to further improve the disturbance rejection performance and tracking accuracy of the radio telescope servo system.

Data Availability

The data used to support the findings of this study are available on request from the corresponding author.

Conflicts of Interest

The authors declare that they have no conflicts of interest.

Acknowledgments

This work was supported by the National Key Research and Development Program of China under grant numbers 2021YFC2203603 and 2021YFC2203501. The research work was also partly supported by the Operation, Maintenance, and Upgrading Fund for Astronomical Telescopes and Facility Instruments, budgeted by the Ministry of Finance of China (MOF), and administrated by the Chinese Academy of Sciences (CAS).

References

[1] J. Q. Cheng, *The Principles of Astronomical Telescope Design*, Springer US, New York, NY, USA, 2009.

[2] F. Fan, H. L. Qian, D. S. Chen, and S. Z. Shen, "Research on key technologies of giant radio telescope structure," *Journal of Building Structures*, vol. 44, no. 4, pp. 129–140, 2023.

[3] N. Wang, Q. Xu, J. Ma et al., "The Qitai radio telescope," *Science China Physics, Mechanics & Astronomy*, vol. 66, no. 8, Article ID 289512, 2023.

[4] W. Gawronski, *Modeling and Control of Antennas and Telescopes*, Springer, Singapore, 2008.

[5] M. Vakil, R. Fotouhi, and P. N. Nikiforuk, "On the zeros of the transfer function of flexible link manipulators and their nonminimum phase behaviour," *Proceedings of the Institution of*

Mechanical Engineers- Part C: Journal of Mechanical Engineering Science, vol. 224, no. 10, pp. 2083–2096, 2010.

[6] W. Gawronski, "Control and pointing challenges of large antennas and telescopes," *IEEE Transactions on Control Systems Technology*, vol. 15, no. 2, pp. 276–289, 2007.

[7] J. Zhang, J. Huang, J. Zhou, C. Wang, and Y. Zhu, "A compensator for large antennas based on pointing error estimation under a wind load," *IEEE Transactions on Control Systems Technology*, vol. 25, no. 5, pp. 1912–1920, 2017.

[8] M. P. Belov and T. H. Phuong, "Servo speed control of the large radio telescope based on linear optimal controller," in *Proceedings of the 2017 XX IEEE International Conference on Soft Computing and Measurements (SCM)*, pp. 352–355, St. Petersburg, Russia, May 2017.

[9] W. Chen and Z. Wang, "Robust control of the servo system of Leighton Chajnantor Telescope under high wind speed," *Modeling, Systems Engineering, and Project Management for Astronomy X*, vol. 12, 2022.

[10] X. Chen, K. Zhou, and Y. Tan, "Revisit of LQG control- A new paradigm with recovered robustness," in *Proceedings of the 2019 IEEE 58th Conference on Decision and Control (CDC)*, pp. 5819–5825, Nice, France, December 2019.

[11] S. Skogestad and I. Postlethwaite, *Multivariable Feedback Control: Analysis and Design*, John Wiley & Sons, Hoboken, NJ, USA, 2005.

[12] E. Sariyildiz, R. Oboe, and K. Ohnishi, "Disturbance observer-based robust control and its applications: 35th anniversary overview," *IEEE Transactions on Industrial Electronics*, vol. 67, no. 3, pp. 2042–2053, 2020.

[13] R. F. A. Khan, K. Rsetam, Z. Cao, and Z. Man, "Singular perturbation-based adaptive integral sliding mode control for flexible joint robots," *IEEE Transactions on Industrial Electronics*, vol. 70, no. 10, pp. 10516–10525, 2023.

[14] K. Rsetam, Z. Cao, and Z. Man, "Design of robust terminal sliding mode control for underactuated flexible joint robot," *IEEE Transactions on Systems, Man, and Cybernetics: Systems*, vol. 52, no. 7, pp. 4272–4285, 2022.

[15] K. Rsetam, Z. Cao, and Z. Man, "Cascaded-extended-state-observer-based sliding-mode control for underactuated flexible joint robot," *IEEE Transactions on Industrial Electronics*, vol. 67, no. 12, pp. 10822–10832, 2020.

[16] K. Rsetam, Z. Cao, L. Wang, M. Al-Rawi, and Z. Man, "Practically robust fixed-time convergent sliding mode control for underactuated aerial flexible JointRobots manipulators," *Drones*, vol. 6, no. 12, p. 428, 2022.

[17] N. Li, N. Wang, Z. Y. Liu, and L. Yang, "Active disturbance rejection-based double-loop control design for large antenna's servo system," *Publications of the Astronomical Society of the Pacific*, vol. 135, no. 1053, Article ID 115001, 2023.

[18] X. Li, W. Zhou, J. Luo, J. Qian, and W. Ma, "High precision position control of telescope servo systems based on active disturbance rejection controller," in *Proceedings of the 2019 Chinese Control Conference*, pp. 3145–3150, CCC, Guangzhou, China, July 2019.

[19] S. Li, J. Yang, W. H. Chen, and X. Chen, "Generalized extended state observer based control for systems with mismatched uncertainties," *IEEE Transactions on Industrial Electronics*, vol. 59, no. 12, pp. 4792–4802, 2012.

[20] Y. Du, W. Cao, J. H. She, M. Wu, M. Fang, and S. Kawata, "Disturbance rejection and control system design using improved equivalent input disturbance approach," *IEEE Transactions on Industrial Electronics*, vol. 67, no. 4, pp. 3013–3023, 2020.

[21] W. R. Chen and Z. Wang, "Disturbance observer-based pointing control of Leighton chajnantor telescope," *Research in Astronomy and Astrophysics*, vol. 24, no. 1, Article ID 015010, 2023.

[22] Q. Wang, H. X. Cai, Y. M. Huang et al., "Acceleration feedback control (AFC) enhanced by disturbance observation and compensation (DOC) for high precision tracking in telescope systems," *Research in Astronomy and Astrophysics*, vol. 16, no. 8, p. 7, 2016.

[23] H. Shim and Y. J. Joo, "State space analysis of disturbance observer and a robust stability condition," in *Proceedings of the 2007 46th IEEE Conference on Decision and Control*, pp. 2193–2198, New Orleans, LA, USA, December 2007.

[24] J. H. She, M. Fang, Y. Ohyama, H. Hashimoto, and M. Wu, "Improving disturbance-rejection performance based on an equivalent-input-disturbance approach," *IEEE Transactions on Industrial Electronics*, vol. 55, no. 1, pp. 380–389, 2008.

[25] P. Yu, M. Wu, J. H. She, K. Z. Liu, and Y. Nakanishi, "Robust tracking and disturbance rejection for linear uncertain system with unknown state delay and disturbance," *IEEE*, vol. 23, no. 3, pp. 1445–1455, 2018.

[26] Y. Du, J. She, and W. Cao, "Improving performance of disturbance rejection for nonlinear systems using improved equivalent-input-disturbance approach," *IEEE Transactions on Industrial Informatics*, vol. 20, no. 1, pp. 941–952, 2024.

[27] Y. Du, W. Cao, J. H. She, M. Wu, M. Fang, and S. Kawata, "Disturbance rejection and robustness of improved equivalent-input-disturbance-based system," *IEEE Transactions on Cybernetics*, vol. 52, no. 8, pp. 8537–8546, 2022.

[28] Z. Wang, J. H. She, Z. T. Liu, and M. Wu, "Modified equivalent-input-disturbance approach to improving disturbance-rejection performance," *IEEE Transactions on Industrial Electronics*, vol. 69, no. 1, pp. 673–683, 2022.

[29] X. Yin, Y. Shi, J. H. She, and Y. Zhang, "Designing low-pass filter in equivalent-input-disturbance compensator for improving disturbance-rejection performance," *ISA Transactions*, vol. 131, pp. 339–348, 2022.

[30] C. C. Wang and M. Tomizuka, "Design of robustly stable disturbance observers based on closed loop consideration using H∞ optimization and its applications to motion control systems," in *Proceedings of the 2004 American Control Conference*, vol. 4, pp. 3764–3769, Boston, MA, USA, July 2004.

[31] E. Daş, "Combined design of robust controller and disturbance observer in a fixed-order H∞ control framework," *Mechatronics*, vol. 88, Article ID 102912, 2022.

[32] X. Yin, J. H. She, M. Wu, D. Sato, and K. Ohnishi, "Disturbance rejection using SMC-based-equivalent-input-disturbance approach," *Applied Mathematics and Computation*, vol. 418, Article ID 126839, 2022.

[33] J. H. She, X. Xin, and T. Yamaura, "Analysis and design of control system with equivalent-input-disturbance estimation," in *Proceedings of the 2006 IEEE International Conference on Control Applications*, Munich, Germany, October 2006.

[34] T. Ranka, M. Garcia-Sanz, A. Symmes, J. M. Ford, and T. Weadon, "Dynamic analysis of the Green Bank Telescope structure and servo system," *Journal of Astronomical Telescopes, Instruments, and Systems*, vol. 2, no. 1, Article ID 014001, 2016.

[35] L. Yang, N. Wang, Z. Liu, and N. Li, "Improving disturbance rejection performance of EID-based control by employing PLTD," *IEEE Access*, vol. 11, pp. 108024–108032, 2023.

[36] H. Kimura, "A new approach to the perfect regulation and the bounded peaking in linear multivariable control systems," *IEEE Transactions on Automatic Control*, vol. 26, no. 1, pp. 253–270, 1981.

[37] C. H. Weng and C. Wen, "Optimal tracking design with robust observer optimization," in *Proceedings of the 2020 39th Chinese Control Conference (CCC)*, pp. 1837–1842, Shenyang, China, July 2020.

[38] K. J. Keesman, *System Identification: An Introduction*, Springer Science & Business Media, New York, NY, USA, 2011.